

Compensation of Random and Systematic Timing Errors in Sampling Oscilloscopes

Paul D. Hale, *Senior Member, IEEE*, C. M. Wang, Dylan F. Williams, *Fellow, IEEE*, Kate A. Remley, *Member, IEEE*, and Joshua Wepman

Abstract--We describe a method of correcting both random and systematic timebase errors using measurements of two quadrature sinusoids made simultaneously with a waveform of interest. We estimate the fundamental limits to our procedure due to additive noise and sampler jitter and demonstrate the procedure with some actual measurements.

Index Terms--jitter, sampling oscilloscope, timebase distortion, waveform metrology, comb generator

I. INTRODUCTION

High-speed sampling oscilloscopes suffer from systematic timebase distortion (TBD) and random jitter that cause errors in the time in a waveform at which samples are acquired. We propose an alternative timebase, for use with conventional sampling oscilloscopes, that greatly reduces both TBD and jitter. The new timebase relies upon simultaneous measurement of the signal of interest, and two reference sinusoids (in quadrature) that serve to determine the actual time at which the measurement was performed [1]. The conventional timebase of the oscilloscope is used to characterize distortion in the two reference sinusoids, and to determine within which half-cycle of the auxiliary sinusoids the signal was measured. The new timebase is estimated from the sinusoids using a weighted “error in variables” approach that accounts for relative contributions of additive noise and timing error.

Sampling oscilloscopes that have a form of jitter correction based on quadrature sinusoidal reference signals are described elsewhere in the literature[2], and sampling oscilloscopes with similar functionality have recently become commercially available[3, 4]. Our implementation achieves the best aspects of these systems simultaneously, including a residual jitter of less than 200 fs, correction of time records with nearly arbitrary length, and it applies to signals at almost any frequency. Furthermore, our method is inexpensive, since it can be implemented with an older

generation of standard equipment. Our method corrects for *both* random jitter and systematic timebase distortion and provides the user with an estimate of the residual timing error after the correction process has been applied. Also our technique is nonproprietary and is described and characterized here, for the first time, in the open archival literature.

In an oscilloscope the timing error at the i th sample, y_i , is the sum of the systematic TBD, h_i , and random timing jitter error \mathbf{t}_i . Thus the i th sample of the signal of interest g , as a function of time, is given by

$$y_i = g(T_i + h_i + \mathbf{t}_i) + \mathbf{e}_i, \quad (1)$$

where $T_i = (i-1)T_s$ is the target time of each sample, T_s is the target time interval between samples, and \mathbf{e}_i is additive noise. We assume the jitter and additive noise are independent zero-mean random variables with variances \mathbf{s}_t^2 and \mathbf{s}_e^2 .

The problem of estimating jitter and correcting for its effects has been addressed by many authors [5,6, 7,8,9]. The typical approach is to obtain the signal variance of independent, repeated measurements and use the approximate model [10]

$$\text{var}(y_i) \approx \mathbf{s}_t^2 (g'(t_i))^2 + \mathbf{s}_e^2 \quad (2)$$

to solve for \mathbf{s}_t^2 . Here $g'(t_i)$ is the derivative of the ideal signal evaluated at $t_i = T_i + h_i$. It is usually assumed that, upon averaging, the jitter acts as a low-pass filter so that the average signal is the convolution of the ideal signal $g(t_i)$ and the probability density function $p(\bullet)$ of the jitter:

$$\langle g(t_i) \rangle = \int g(t_i - \mathbf{t}) p(\mathbf{t}) d\mathbf{t}. \quad (3)$$

The effects of jitter are then removed by deconvolution [5].

This approach has the following problems:

- Measurements must be repeated to find the measurement mean and variance.
- Estimates of the jitter variance from (2) are generally biased (for example, see [9]).
- $p(\bullet)$ must be known.
- $p(\bullet)$ must be the same over the entire measured waveform.
- The averaging process removes some of the inherent bandwidth from the measured signal, making the deconvolution subjective[11, 12].

P. D. Hale is with the Optoelectronics Division, National Institute of Standards and Technology, Boulder, CO, 80305 USA (e-mail: hale@boulder.nist.gov).

C. M. Wang is with the Statistical Engineering Division, National Institute of Standards and Technology, Boulder, CO, 80305 USA.

D. F. Williams, K. A. Remley, and J. Wepman are with the Electromagnetic Technology Division, National Institute of Standards and Technology, Boulder, CO, 80305 USA.

Publication of the U. S. Government, not subject to U.S. copyright.

- f) Deconvolution is an “ill-posed” problem [12], so that in the presence of noise there is no unique solution.

Generally, it is desirable to avoid deconvolution, particularly in cases where the jitter is large, varies over the measurement time window, or has a non-Gaussian probability density. All these situations make deconvolving the jitter from (3) problematic.

The problem of estimating TBD has also been studied by many authors [13- 20]. Recent work [17- 20] has used a nonlinear least-squares approach that fits multiple measured sinusoids with multiple phases and frequencies to a distorted sinusoid model. This approach performs well at discontinuities in the TBD and allows simultaneous estimation of the harmonic distortion, if any, in the measured sinusoids. The distorted-sinusoid model, with harmonic number n_h , is given by [18]

$$y_{ij} = \mathbf{a}_j + \sum_{k=1}^{n_h} \left[\mathbf{b}_{jk} \cos(2pkf_j t_{ij}) + \mathbf{g}_{jk} \sin(2pkf_j t_{ij}) \right] + \mathbf{e}_{ij}, \quad (4)$$

where f_j is the fundamental frequency of the j th measured waveform y_{ij} at the i th nominal time, $t_{ij} = T_i + h_i + \mathbf{t}_{ij}$. The random jitter is \mathbf{t}_{ij} and \mathbf{e}_{ij} is random additive noise. The values of \mathbf{a}_j , \mathbf{b}_{jk} , \mathbf{g}_{jk} , and h_i can be estimated, by use of a weighted least-squares approach [18]. To obtain a solution using this approach, we typically measure a set of sinusoidal waveforms at two or three different frequencies. Each set includes two sinusoids, of a given frequency, that are approximately in quadrature. Hence, each set can have up to four or six waveforms. When estimating TBD we generally average over several measurement sets to reduce the uncertainty due to random jitter and additive noise.

In the present work, however, we are interested in the *total* timebase error, i.e. the sum of the TBD and the jitter. We use all of the information in the sinusoid to find the distortion (that is, we estimate \mathbf{a}_j , \mathbf{b}_{jk} , and \mathbf{g}_{jk}) and the

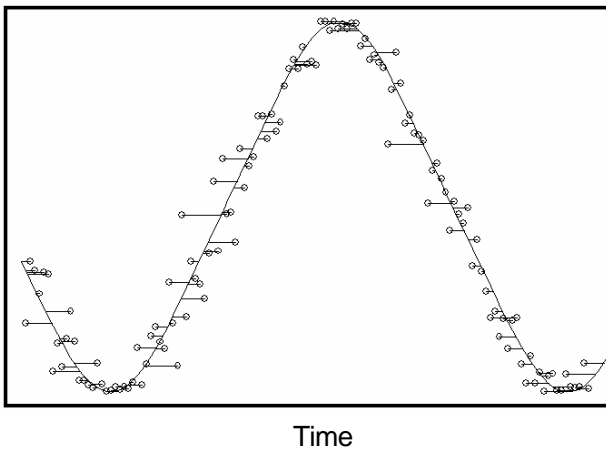


Figure 1. Circles show sampled signal using distorted and jittered oscilloscope timebase and the solid curve shows the estimated distorted sinusoid. Horizontal lines show difference between the time estimated from the curve and the nominal oscilloscope timebase.

timebase (h_i and \mathbf{t}_{ij}) simultaneously so that the measured dependent variable (y_{ij}) best corresponds to the values of the distorted reference sinusoids with the new timebase. In this case, no averaging is involved.

A simple illustration is shown in Fig. 1, which plots uncorrected measurements (circles at time T_i) of a reference sinusoid with an estimate of the distorted sinusoid (solid curve). The estimated sinusoid is found by minimizing the average “distance” between the samples and the sinusoid. If we assume, for illustrative purposes, that there is no additive noise, we can estimate the total time error due to timebase distortion and jitter by drawing a horizontal line between each measurement (circles) and the distorted sinusoid. The length of each line represents the difference between the nominal (oscilloscope) time at which the measurement was taken and the time as determined by the distorted sinusoidal fit. The time that each line intersects the distorted sinusoid is the corrected time for each sample. Once the timebase error is known, it can be applied to a simultaneously measured signal of interest if the timing errors of the simultaneous measurements are sufficiently correlated.

II. SYSTEM FOR MEASURING AND CORRECTING TIMEBASE ERRORS

Fig. 2 shows a generalized schematic of the signal generator and sampling system for correcting timebase errors. The reference oscillator generates a sinusoid with frequency f . The waveform generator and trigger generator are synchronized to the reference oscillator.

We take advantage of the parallel design of many equivalent-time sampling oscilloscopes. In such an oscilloscope, the sampling process proceeds as follows [21,15]: (a) the timebase is armed to trigger on a rising or falling edge at a certain level, (b) a pulse with the desired

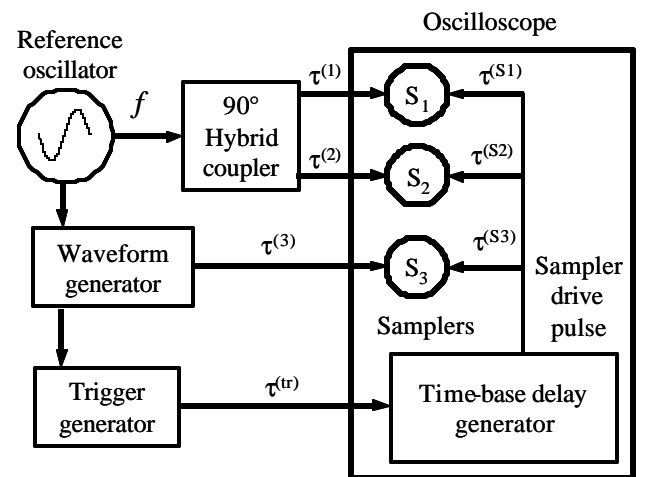


Figure 2. Schematic diagram of generic system used to measure and correct oscilloscope timebase errors. The reference generator, waveform generator, and trigger generator are synchronized. Various sources of jitter are labeled as $\tau^{(*)}$.

characteristics is sent into the trigger input, triggering the timebase, (c) the timebase (delay generator) waits for a predefined time delay, and then (d) the timebase generates a drive (strobe) pulse that is split and sent simultaneously to *all* the samplers in the oscilloscope mainframe. A waveform is sampled by incrementing the time delay by a nominal increment T_s and repeating the process. A result of the parallel architecture is that any jitter on the trigger pulse or the timebase delay generator is common to the sampling time of *all* the samplers in the oscilloscope mainframe.

In Fig. 2 we show the sources of jitter, measured relative to an absolute reference oscillator. They include $\mathbf{t}^{(1)}$ and $\mathbf{t}^{(2)}$, which are the jitter of the reference signals.

We expect that these have the same statistical properties (mean of 0 and standard deviation $\mathbf{s}^{(1)} = \mathbf{s}^{(2)}$), although their individual realizations for the i th sample will differ. The value of $\mathbf{t}^{(3)}$ is the jitter of the generated waveform we want to measure and has mean 0 and standard deviation $\mathbf{s}^{(3)}$. The value of $\mathbf{t}^{(tr)}$ is the jitter of the trigger generator and timebase generator circuit and has mean 0 and standard deviation $\mathbf{s}^{(tr)}$. We also include a jitter \mathbf{t}^{Sx} ($x=1, 2, 3$) for the actual sampling process for each of the samplers, with mean 0 and standard deviation $\mathbf{s}^{(S1)} \simeq \mathbf{s}^{(S2)} \simeq \mathbf{s}^{(S3)}$.

When the samplers are simultaneously fired from the same trigger event, the different jitter components contribute to the sampled signals as follows:

$$\begin{aligned} S_1(t_i) &= S_1(T_i + h_i + \mathbf{t}_i^{(1)} + \mathbf{t}_i^{(S1)} + \mathbf{t}_i^{(tr)}) \\ S_2(t_i) &= S_2(T_i + h_i + \mathbf{t}_i^{(2)} + \mathbf{t}_i^{(S2)} + \mathbf{t}_i^{(tr)}) \\ S_3(t_i) &= S_3(T_i + h_i + \mathbf{t}_i^{(3)} + \mathbf{t}_i^{(S3)} + \mathbf{t}_i^{(tr)}) \end{aligned} \quad (5)$$

We note that h_i and $\mathbf{t}_i^{(tr)}$ are common to all the simultaneously sampled waveforms. Hence, if $\mathbf{s}^{(tr)} \gg \mathbf{s}^{(x)}$ and $\mathbf{s}^{(tr)} \gg \mathbf{s}^{(Sx)}$ ($x=1, 2, 3$), $\mathbf{t}_i^{(tr)}$ is the dominant source of jitter and we can approximate \mathbf{t}_{ij} as $\mathbf{t}_i^{(tr)}$. Furthermore, if we can estimate h_i and $\mathbf{t}_i^{(tr)}$ from the known sinusoidal signals $S_1(t_i)$ and $S_2(t_i)$, we can apply our estimate to the third waveform, $S_3(t_i)$, and compensate for timing errors in its measurement.

III. ESTIMATING RANDOM JITTER

Our approach to estimating the timing errors in (4) is to apply the so called errors-in-variables [22] or orthogonal distance regression (ODR) [23] to the model in (4). In this approach, the distorted sinusoid model is fit to the data with the assumption that both “dependent” (y_i) and “independent” (t_{ij}) variables are subject to errors. Specifically, let y_{i1} and y_{i2} be the i th samples of nearly quadrature sinusoids measured simultaneously with the signal of interest. Denote the total timing error as $\mathbf{d}_{ij} = h_i + \mathbf{t}_{ij}$, $j=1, 2$. Then \mathbf{d}_{i1} and \mathbf{d}_{i2} are the timing errors of the two sinusoid measurements. Because the strobe pulse drives all the samplers nearly simultaneously,

as described in the previous section, we assume equal timing errors in channels 1 and 2. That is, we assume $\mathbf{t}_{i1} = \mathbf{t}_{i2} = \mathbf{t}_i$, and hence $\mathbf{d}_i = \mathbf{d}_{ij} = h_i + \mathbf{t}_i$ and $t_i = t_{ij} = T_i + \mathbf{d}_i$. We rewrite y_{ij} , given in (4), as a function F of $\mathbf{q}_j = (\mathbf{a}_j, \mathbf{b}_{j1} \dots \mathbf{b}_{jn_h}, \mathbf{g}_{j1} \dots \mathbf{g}_{jn_h})$ as

$$y_{ij} = F(T_i + \mathbf{d}_i; \mathbf{q}_j) + \mathbf{e}_{ij}.$$

Estimates of timing errors \mathbf{d}_i are readily available from the ODR fit of the model using ODRPACK [23]. The ODR procedure obtains the best-fit model for this problem by minimizing

$$\begin{aligned} E(\mathbf{q}_1, \mathbf{q}_2, \mathbf{d}_i) &= \sum_{i=1}^n w_e (\mathbf{e}_{i1}^2 + \mathbf{e}_{i2}^2) + w_d \mathbf{d}_i^2 \\ &= \sum_{i=1}^n \left\{ w_e \left([F(T_i + \mathbf{d}_i; \mathbf{q}_1) - y_{i1}]^2 + [F(T_i + \mathbf{d}_i; \mathbf{q}_2) - y_{i2}]^2 \right) + w_d \mathbf{d}_i^2 \right\} \end{aligned}$$

with respect to $\mathbf{q}_1, \mathbf{q}_2$, and $\{\mathbf{d}_i, i=1, \dots, n\}$, where n is the number of samples. The relative weight for errors \mathbf{e} and \mathbf{d} , is denoted by $w = w_e / w_d$ and the timing error estimate is optimized when $w = \mathbf{s}_t^2 / \mathbf{s}_e^2$ [23].

This ODR approach works well for most of the data we observe in our laboratory and requires only two nearly quadrature sinusoids. There are instances, however, where the ODR approach produces unsatisfactory results. This is the case, for example, when the waveform is very long or there are only a few samples per cycle of the sinusoid. In such cases, we use an estimate of the TBD as an initial guess for the total timebase error to help the ODR routine converge to a solution. This initial TBD estimate requires additional measurements of quadrature sinusoids at different frequencies. These additional measurements need not be made simultaneously with the signal of interest.

IV. SIMULATION STUDIES

Additive noise on the reference sinusoids can be a source of error in any time-base error correction. From (2) we see that the frequency f of the sinusoid $g(t)$ should be chosen such that $\mathbf{s}_t^2 (g'(t))^2 \gg \mathbf{s}_e^2$ over most of the sinusoid. That is, to achieve good discrimination between jitter noise and additive noise, the slew rate must be high enough so that the jitter noise becomes the dominant noise process for most of the sinusoid. For our sinusoid, we require $\mathbf{s}_t^2 (2\pi f A)^2 \gg \mathbf{s}_e^2$, where A is the amplitude of the sine wave.

We can estimate the root-mean-square (RMS) residual error \mathcal{S}_Δ due to additive noise, in the limit of zero jitter, as $\mathcal{S}_\Delta = (2\pi f)^{-1} (\mathbf{s}_e / A)$. For a 10 GHz sinusoid and $100(\mathbf{s}_e / A) = 0.1\%$, $\mathcal{S}_\Delta = 0.016\text{ps}$. We expect the proposed method will achieve lower residual timing error

Table 1. Amplitude of fundamental and harmonics used in the simulation study

Fundamental frequency, GHz	Harmonic amplitude, V		
	Fundamental	Second harmonic	Third harmonic
10.0000	0.150	0.0006	0.007
9.8855	0.150	0.0006	0.007
10.2855	0.150	0.0002	0.0003

because optimum weighting is used to account for the presence of both jitter and additive noise.

We used simulation to investigate the proposed method for estimating the timing error and the fundamental limits imposed by additive noise. The criterion used in the comparisons is the amount of timing error remaining in a waveform of interest after both random and systematic timebase errors were corrected using the estimation procedure.

Recall that

$$t_{ij} = T_i + h_i + \mathbf{t}_{ij}.$$

With estimates (denoted by $\hat{\cdot}$) of the TBD, \hat{h}_i , and jitter, $\hat{\mathbf{t}}_{ij}$, obtained by the estimation procedure, the best estimate of t_{ij} is then given by

$$\hat{t}_{ij} = T_i + \hat{h}_i + \hat{\mathbf{t}}_{ij}.$$

The remaining timing errors can be characterized by the standard deviation, \mathbf{s}_Δ , of

$$\Delta_{ij} = t_{ij} - \hat{t}_{ij} = h_i + \mathbf{t}_{ij} - (\hat{h}_i + \hat{\mathbf{t}}_{ij}),$$

where h_i and \mathbf{t}_{ij} are the actual TBD and jitter used in the simulation.

We generated sinusoids according to (4) to simulate actual measurements. The simulation parameters used here, including TBD, are closely related to those we observe in our laboratory. We used a time-measurement window (waveform epoch) of 52 ns with 53248 samples. Since the TBD is large for this long time record, we estimated TBD and used it as an initial guess for the total time error. We generated 100 sets of 6 sinusoids, including 0° and 90° phases at three different frequencies. The signal frequencies and amplitudes are given in Table 1, along with the amplitude of the harmonics ($n_h=3$). In each simulation experiment, the additive noise \mathbf{e}_{ij} was generated using a normal distribution with mean 0 and standard deviation \mathbf{s}_t . The random jitter \mathbf{t}_{ij} was generated using a normal distribution with mean 0 and standard deviation \mathbf{s}_e . We also saved the nominal realization of \mathbf{t}_{ij} for the purpose of calculating Δ_{ij} and \mathbf{s}_Δ .

Table 2 displays the mean value of \mathbf{s}_Δ (from the 100 simulations) of the 10 GHz 0° sinusoids for each of the combinations of \mathbf{s}_e and \mathbf{s}_t used in the simulation experiments, with the standard deviation of \mathbf{s}_Δ from the 100 simulations in parentheses. Table 2 shows that our

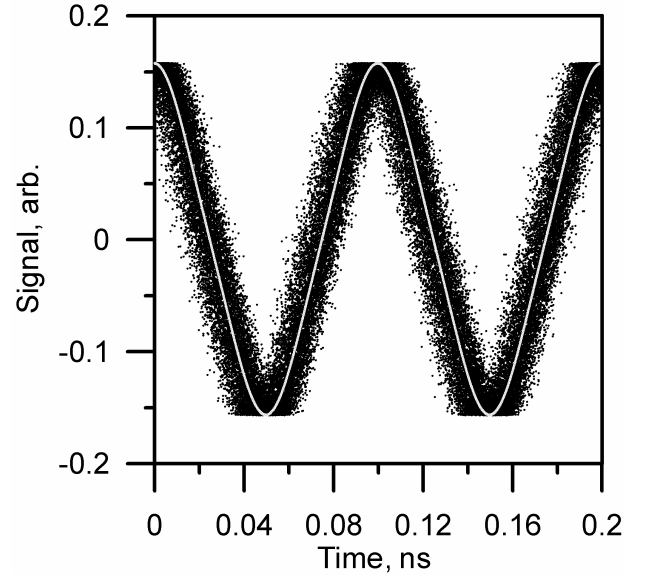


Figure 3. Plot of one of the 52 ns long 10 GHz 0° sinusoids with (light dots) and without (black dots) correcting timing errors. See text for explanation.

procedure is effective for correcting the timing errors even in the presence of additive noise. The additive noise has a relatively large effect on the residual jitter, while the original jitter has a relatively small effect, as shown by the similar values in each row of Table 2. Using the optimum weighting allows us to achieve residual timing errors that are comparable to or below the simple estimate \mathbf{s}_Δ described at the beginning of this section. The small standard deviations in the simulations show that the algorithm gives results that are repeatable to within a few femtoseconds.

We plot one of the simulated 10 GHz 0° sinusoids with and without correcting the timing errors in Fig. 3. The long waveform (520 periods in our simulated experiments)

Table 2. Simulated residual timing errors, \mathbf{s}_Δ (in picoseconds), along with standard deviation of the simulation (in parentheses) as a function of additive noise and random jitter standard deviations \mathbf{s}_e and \mathbf{s}_t . Simulation conditions are described in Section IV. The relative weights are $w = \mathbf{s}_t^2 / \mathbf{s}_e^2$, except when $\mathbf{s}_t = 0$, where $w = 10^{-5}$.

\mathbf{s}_e , % of amplitude	\mathbf{s}_Δ , ps			
	\mathbf{s}_t , ps			
	0ps	1.6 ps	3.2 ps	6.4 ps
0.1	0.009 (0.000)	0.020 (0.003)	0.021 (0.004)	0.022 (0.003)
1	0.091 (0.000)	0.161 (0.001)	0.165 (0.003)	0.187 (0.011)
5	0.456 (0.001)	0.747 (0.002)	0.789 (0.002)	0.806 (0.003)

is shown as a series of overlapping short waveforms (2 periods in this example), similar to an eye pattern. The widely scattering points are the sinusoid generated with $\mathbf{s}_t = 3.2$ ps and $\mathbf{s}_e = 1\%$ of the amplitude. The overlaying (lightly shaded) points are the sinusoid after correction for timebase errors. It is clear from Fig. 3 that after correction, the errors have been collapsed to such a small level that they can not be resolved on this scale.

We next consider the effects of using the incorrect harmonic order in the estimation procedure. In general, the harmonic distortion that is not accounted for will have the same effect as having an inflated additive noise, with the magnitude of the effect depending on the magnitude of the distortion that is not accounted for. For example, if we simulate the actual nominal signal with $\mathbf{s}_t = 3.2$ ps, $\mathbf{s}_e = 1\%$, but $n_h = 5$, and with the amplitudes of the actual 4th and the 5th harmonics equal to those of the 2nd and the 3rd, while we use only three harmonic terms to correct the timing errors, the mean value of \mathbf{s}_Δ (for 100 simulations) is found to be 1.167 ps, a substantial increase from the mean of 0.165 ps (given in Table 2). However, if harmonic distortion in the 4th and the 5th is negligible we do not see a substantial increase. For example, if the amplitudes of the 4th harmonic for all three frequencies are all 0.1 mV, and the amplitudes of the 5th harmonic of the three frequencies are 0.7 mV, 0.7 mV, and 0.1 mV, then the resulting mean value of \mathbf{s}_Δ is only 0.196 ps. It is therefore necessary to have some knowledge of the number of harmonics, n_h , to include in the distorted sinusoid model of (4), as was done in [18].

V. EXPERIMENTAL STUDY

In this section we describe experiments that verify our compensation technique. We also provide example measurements where timebase correction is particularly important, including cases with large jitter or long time windows where TBD can give significant errors.

A. Experimental Study 1: A single sinusoid

We tested the assumption, that the trigger and timebase generator are the dominant sources of jitter ($\mathbf{s}^{(tr)} \gg \mathbf{s}^{(s)}$), which is necessary for this method to be useful, by measuring an “unknown” sinusoid (on sampler 3 of Fig. 2) that was split from the 10 GHz reference signal generator using a 3 dB splitter. The other output of the splitter was further split in a hybrid coupler to provide 0° and 90° reference signals to samplers 1 and 2 of Fig. 2. The reference signals were provided by the clock output of a digital pattern generator and the oscilloscope was triggered at 1/16 of the clock frequency using the trigger output of the pattern generator. After measuring 50 sets of these 3 sinusoids, we changed the reference frequency to the others listed in Table 1 and measured 50 sets of 0° and 90° sinusoids at those frequencies as well. Using the jitter estimation software in the oscilloscope, we estimated the jitter of the uncorrected measurement to have standard

deviation of about 3.3 ps. From a separate measurement, with no input to samplers 1 and 2, we found the RMS additive noise was about 0.3% of the reference signal amplitude.

Because the sinusoid to be corrected and the reference signals are derived from the same source, we expect that the jitter errors $\mathbf{t}_i^{(1)}$, $\mathbf{t}_i^{(2)}$, and the jitter error $\mathbf{t}_i^{(3)}$ of the “unknown” sinusoid are highly correlated and, therefore, nearly equal. Hence, we expect this experiment to be insensitive to these parameters, with the remaining jitter being predominantly due to the jitter \mathbf{t}^{Sx} ($x = 1, 2, 3$) in the samplers.

We estimated the timing errors in this experiment using $n_h = 3$ and used measurements at all three frequencies to calculate the TBD as an initial guess for the ODR routine. Figure 4 shows a section of five of the 10 GHz sinusoids measured by the third sampler before (bottom) and after (top) correction for timebase errors. The uncorrected measurement has a discontinuity at 4 ns, due to timebase distortion, and the random noise is large where the slope is large, indicating significant jitter in the measurement. The corrected sinusoids have the discontinuity removed and exhibit noise that is greatly reduced and evenly distributed in time. Note that the waveforms shown in Fig. 4 have *not* been averaged.

We cannot use the procedure described in Section IV to evaluate the residual timing error because, for experimental data, both h_i and \mathbf{t}_{ij} are unknown. If the waveforms of interest are sinusoidal, however, we can use the ODR procedure [23] to obtain an estimate of the residual timing error after correction. This is obtained from a sum of squares of the residuals of the ODR fit in the “independent” (t_{ij}) variable. The mean of the 50 standard

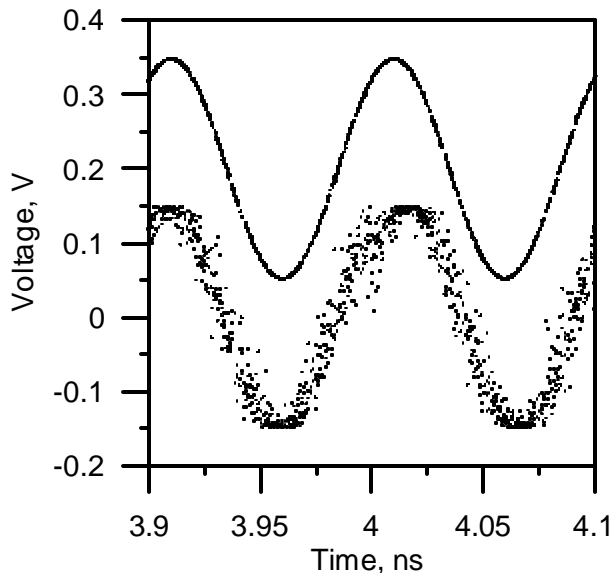


Figure 4. Portion of five sinusoids measured on sampler 3 before (bottom) and after (top) correction for time-base errors. The offset between the curves has been added for clarity.

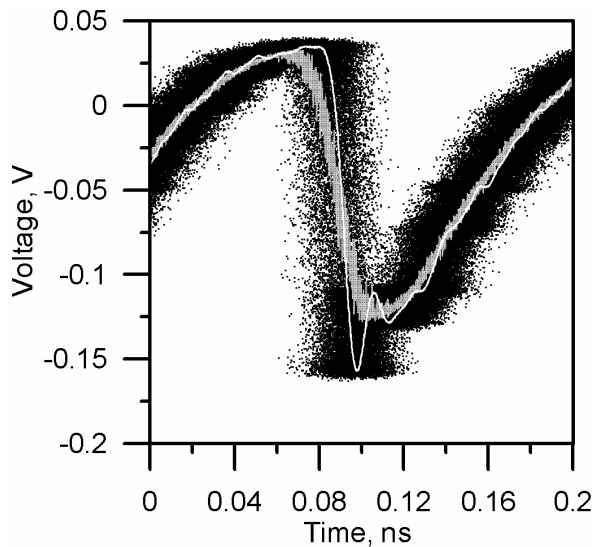


Figure 5. Comparison of raw measurement (black dots), averaged measurement (noisy gray line), and timebase-corrected and averaged measurement (smooth light line).

deviations of the residuals in \hat{t}_i obtained from the ODR fit to the sinusoids measured in sampler 3 was found to be 0.2 ps. Thus, our experimental results show a jitter considerably larger than the numerical results of Table 2, and we can conclude that the jitter $t^{(S)}$ of the samplers is *not* negligible but is still much smaller than the original jitter in the measurement. We estimated the jitter of one of the samplers, using the estimated limit of 0.051 ps from Table 2, as $\sqrt{0.2^2 - 0.021^2} / \sqrt{2} = 0.14$ ps, giving an estimated fundamental limit to our timebase correction. We divide by $\sqrt{2}$ to reflect the simplification that the residual sampler jitter is evenly distributed between sampler 3 and

the sampler that is predominantly used as the reference signal for any given sample.

B. Experimental Study 2: Fast transient with jitter

In some measurement situations, jitter may blur details of a fast transient event, such as the output of a comb generator used for calibrating various high-speed measurement equipment. To demonstrate our timebase correction in this application, we used a 6 GHz signal generator to drive a nonlinear transmission line (NLTL). The NLTL was configured to steepen the falling edge of the generated sinusoid, giving a fast transient with a 6 GHz repetition rate. The output of the signal generator was split between a countdown trigger generator, used to trigger the oscilloscope, the NLTL, and a hybrid coupler whose outputs were used as the reference signals on samplers 1 and 2. The measured transient from the NLTL has roughly a 9 ps fall time.

By changing the trigger level of the oscilloscope we can change the root mean square (rms) jitter from about 1.4 ps to more than 8.6 ps (as measured by the oscilloscope). Additive noise on the reference signals was about 0.4% of the sinusoid amplitude. Figure 5 shows 50 measurements of the waveform generated by the NLTL before averaging (black dots) and after averaging (noisy gray line) for the case where the rms jitter is 8.6 ps. The light smooth curve in Fig. 5 is the result of the following correction and averaging procedure: (a) each of the 50 waveforms was corrected for timebase errors, (b) each corrected waveform was linearly interpolated back to the original evenly spaced time grid, and (c) the resulting curves were averaged. This estimated waveform has much less noise but has ripple, ringing, and sharp features that are blurred in the corresponding average of the uncorrected measurements.

Figure 6 shows an expanded view of the waveform after applying our procedure, with three different

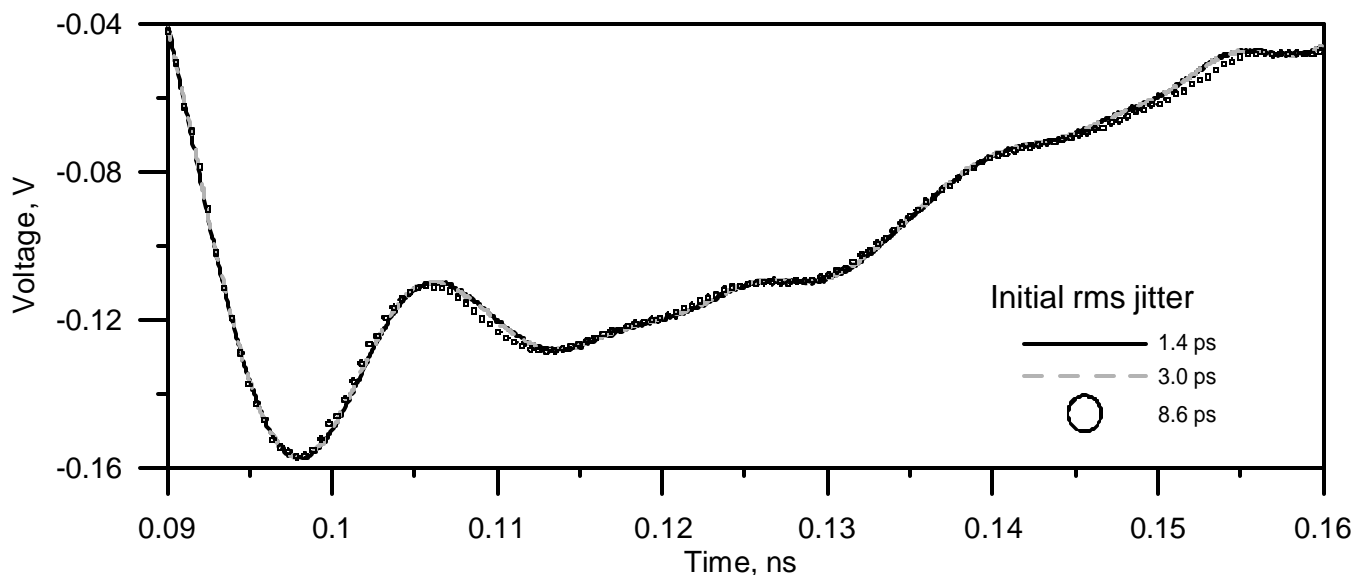


Figure 6. Comparison of some corrected and averaged measurements. Measurements with initial jitter of 1.4 ps and 3.0 ps are indistinguishable on this scale, while the measurement with initial jitter of 8.6 ps shows differences as large as 1.4 ps at some times.

Table 3. Residual jitter on measured NLTL waveform

Initial rms jitter (as measured on oscilloscope), ps	Residual rms jitter (after correction, $w = s_t^2/s_e^2$), ps
1.4	0.15
3.0	0.20
6.3	0.25
8.6	0.25

initial values of jitter. Notice that the curves lie nearly on top of each other. Because the ringing and ripple are accurately represented in each reconstructed waveform, these features are *not* artifacts of the signal processing, as might be expected with some kinds of regularized noncausal deconvolution [11].

Closer inspection of the curves in Fig. 6 shows systematic time differences in the curves that increase with initial jitter, but are still substantially less than the initial jitter. The two lowest jitter curves typically agree to within 100 fs, while the lowest and highest jitter cases differ by as much as 1.1 ps at some times. The cause of the systematic difference between the high and low jitter cases is unknown at this time. The calculated fall times (10-90% of peak-to-peak transition durations) of all four cases are indistinguishable.

Because we do not have an analytic expression for the fast transient, we cannot use the ODR approach to estimate the residual timing error in its measurement after correction. To estimate the residual jitter in the transient measurement we used (2) on the corrected and linearly interpolated waveforms. Interpolation to a uniform grid allows us to estimate the variance and derivative at a given time, as is needed in (2). The results of our estimate are shown in Table 3. We observe that the results for the experiments with most similar initial jitter (3.2 ps in sinusoidal experiment, 3.0 ps in NLTL experiment) are in good agreement; both have 0.2 ps residual jitter after correction and include the same amount of error from sampler jitter. Table 3 also shows that the resulting residual jitter is only weakly dependent on the initial jitter, as expected from the simulations in Section IV, and that the algorithm can improve a high jitter measurement by as much as 34× (from 8.6 ps to 0.25 ps).

VI. DEMONSTRATION PROGRAM

Our program for post-processing acquired waveforms for timebase correction has a graphical user interface. The program is available at http://www.boulder.nist.gov/div815/HSM_Project/HSMP.htm.

VII. CONCLUSION

We have shown how to simultaneously estimate the systematic and random timebase errors of measured sinusoidal reference signals. Using the parallel (simultaneous) sampling in our oscilloscope allows us to

use this estimate to correct the timebase errors in a simultaneously measured waveform by roughly a factor of 10, effectively replacing the timebase of the oscilloscope with a timebase provided by the measured sinusoids. We require only that the oscilloscope timebase have enough accuracy to allow us to discriminate between consecutive cycles of the clock signal. This allows us to correct the timing errors that might be present with long waveforms or large jitter, and lowers the noise floor significantly in most measurements without averaging. In addition to the examples described in this paper, we have also demonstrated clear reduction of effects due to random jitter and timebase distortion in measurements of 10 Gbit/s data sequences that are 52 ns (53248 samples) long and multisine signals that are 500 ns (40960 samples) long.

VIII. ACKNOWLEDGEMENTS

We gratefully acknowledge the loan of the NLTL by Martin Van Pelt, and help with generating the Dynamic link libraries (DLLs) for the Visual Basic interface from Abbie O’Gallagher. We also thank Tracy Clement, Jonathan Scott, and Don Larson for detailed review of our manuscript.

- [1] S. H. Pepper, “Synchronous sampling and applications to analytic signal estimation,” *56th ARFTG Conf. Dig.*, pp.170-179, Dec. 2000.
- [2] R. L. Jungerman, G. Lee, O. Buccafusca, Y. Kaneko, N. Itagaki, R. Shioda, A. Harada, Y. Nihei, and G. Sucha, “1-THz Bandwidth C- and L-band optical sampling with a bit rate agile timebase,” *IEEE Photon. Technol. Lett.*, vol. 14, pp. 1148-1150, 2002.
- [3] Agilent 86107A precision timebase reference module. NIST does not endorse or guarantee this product. This product is listed here only to reference similar measurement techniques. Other products may perform as well or better than those listed here.
- [4] Tektronix 82A04 phase reference module. NIST does not endorse or guarantee this product. This product is listed here only to reference similar measurement techniques. Other products may perform as well or better than those listed here.
- [5] W. L. Gans, “The measurement and deconvolution of time jitter in equivalent-time waveform samplers,” *IEEE Trans. Instrum. Meas.*, vol. 32, pp. 126-133, 1983.
- [6] J. Verspecht, “Compensation of timing jitter-induced distortion of sampled waveforms,” *IEEE Trans. Instrum. Meas.*, vol. 43, pp. 726-732, 1994.
- [7] G. Vandersteen and R. Pintelon, “Maximum likelihood estimator for jitter noise models,” *IEEE Trans. Instrum. Meas.*, vol. 49, pp. 1282-1284, 2000.
- [8] M. G. Cox, P. M. Harris, and D. A. Humphreys, “An algorithm for the removal of noise and jitter in signals and its application to picosecond electrical measurement,” *Numerical Algorithms*, 5, pp. 491-508, 1993.
- [9] K. J. Coakley, C. M. Wang, P. D. Hale, and T. S. Clement, “Adaptive characterization of jitter noise in sampled high-speed signals,” *IEEE Trans. Instrum. Meas.*, vol. 52, pp. 1537-1547, 2003.
- [10] T. M. Souders, D. R. Flach, C. Hagwood, and G. L. Yang, “The effects of timing jitter in sampling systems,” *IEEE Trans. Instrum. Meas.*, vol. 39, pp. 80-85, 1990.
- [11] N. S. Nahman and M. E. Guillaume, *Deconvolution of Time Domain Waveforms in the Presence of Noise*, NBS Technical Note 1047, National Bureau of Standards, Oct. 1981.
- [12] *Solutions of ill-posed problems*, A. N. Tikhonov and V. Y. Arsenin, V. H. Winston and Sons, Washington, D. C., 1977.

-
- [13] W. R. Scott Jr., "Error corrections for an automated time-domain network analyzer," *IEEE Trans. Instrum. Meas.*, vol. 35, pp. 300-303, 1986.
- [14] J. Verspecht, "Accurate spectral estimation based on measurements with a distorted-timebase digitizer," *IEEE Trans. Instrum. Meas.*, vol. 43, pp. 210-215, 1994.
- [15] J. B. Retting and L. Dobos, "Picosecond time interval measurements," *IEEE Trans. Instrum. Meas.*, vol. 44, pp. 284-287, 1995.
- [16] "IEEE standard for digitizing waveform recorders," IEEE Std. 1057-1994, 1994.
- [17] G. N. Stenbakken and J. P. Deyst, "Timebase nonlinearity determination using iterated sine-fit analysis," *IEEE Trans. Instrum. Meas.*, vol. 47, pp. 1056-1061, 1998.
- [18] C. M. Wang, P. D. Hale, and K. J. Coakley, "Least-squares estimation of timebase distortion of sampling oscilloscopes," *IEEE Trans. Instrum. Meas.*, vol. 48, pp. 1324-1332, 1999.
- [19] G. Vandersteen, Y. Rolain, and J. Schoukens, "An identification technique for data acquisition characterization in the presence of nonlinear distortions and timebase distortions," *IEEE Trans. Instrum. Meas.*, vol. 50, pp. 1355-1363, 2001.
- [20] C. M. Wang, P. D. Hale, K. J. Coakley, and T. S. Clement, "Uncertainty of oscilloscope timebase distortion estimate," *IEEE Trans. Instrum. Meas.*, vol. 51, pp. 53-58, 2002.
- [21] J. Verspecht, "Calibration of a measurement system for high frequency nonlinear devices," Ph.D. Thesis, Free University of Brussels, Brussels, Belgium, Sept. 1995.
- [22] W. A. Fuller, *Measurement error models*, NY: John Wiley, 1987.
- [23] P. T. Boggs, R., H. Byrd, J. E. Rogers, and R. B. Schnabel, "User's reference guide for ODRPACK version 2.01 software for weighted orthogonal distance regression," Nat. Inst. Stand. Technol. Internal Report, NISTIR 92-4834, June 1992.